Inducing Propulsion of Colloidal Dimers by Breaking the Symmetry in Electrohydrodynamic Flow

Fuduo Ma,[1] Xingfu Yang,[1] Hui Zhao,[2] and Ning Wu[1,*]
[1]Department of Chemical and Biological Engineering, Colorado School of Mines, Golden, Colorado 80401, USA
[2]Department of Mechanical Engineering, University of Nevada, Las Vegas, Nevada 89154, USA
(Received 21 July 2015; revised manuscript received 2 October 2015; published 10 November 2015)

We show that dielectric colloidal dimers with broken symmetry in geometry, composition, or interfacial charges can all propel in directions that are perpendicular to the applied ac electric field. The asymmetry in particle properties ultimately results in an unbalanced electrohydrodynamic flow on two sides of the particles. Consistent with scaling laws, the propulsion direction, speed, and orientation of dimers can be conveniently tuned by frequency. The new propulsion mechanism revealed here is important for building colloidal motors and studying collective behavior of active matter.

DOI: 10.1103/PhysRevLett.115.208302 PACS numbers: 82.70.Dd

The autonomous propulsion and active transport of microscopic objects in a fluidic environment are essential for maintaining the bioactivities of all living species [1,2]. Artificial colloidal motors that can deliver cargoes on demand could revolutionize many modern technologies including targeted drug delivery [3,4], microrobots [5,6], intelligent sensors [7], and miniaturized surgeries [8]. Because of the low Reynolds number, conventional swimming strategies that rely on inertia do not work [9,10]. Instead, one needs to break the system symmetry and fluid flow. For example, when a metallodielectric (e.g., gold-polystyrene) Janus sphere is subjected to an ac electric field, it propels in directions that are perpendicular to the field [11,12]. This phenomenon is different from conventional electrophoresis and dielectrophoresis [13], where the electric field usually dictates particles' trajectories either along the field line or toward the field gradient. The particle motion has been attributed to the induced-charge electro osmosis (ICEO) [14]. The external field induces ions and generates much stronger electro-osmotic flow along the gold surface than on the polystyrene side. As the result of unbalanced liquid flow, the Janus sphere moves with its dielectric hemisphere oriented forward.

One outstanding question addressed here is whether more general types of asymmetry in particle properties can lead to locomotion, especially for purely dielectric particles, where ICEO is typically negligible. It is known that, under a perpendicular ac field, dielectric spheres can aggregate laterally into close-packed arrays due to a tangential electrohydrodynamic (EHD) flow [15,16]. Although much effort has been spent to understand the origin of this flow [17–19] and to exploit it for assembly [20,21], little attempt has been made to break the symmetry of EHD flow for particle propulsion except our recent observation that chiral clusters assembled from colloidal dimers can rotate according to their handedness [22]. Here we show that one can rationally tailor colloidal particles with broken symmetry in geometric, compositional, or interfacial properties, all of which create an unbalanced EHD flow and lead to particle propulsion.

To make dimers with well-controlled broken symmetry, we employ the "salt-in-salt-out" method [23]. In brief, spheres of type A and type B are mixed in 0.01 M potassium chloride (KCl) solution. Because of the screening of double-layer repulsion, particles aggregate irreversibly. By controlling both particle concentration and aggregation time, we obtain a mixture of aggregates that primarily consists of individual spheres and dimers (AB, AA, and BB). The aggregates remain stable after being washed in deionized water several times. They are then redispersed in aqueous solution with specific salt concentrations. This method allows us to accurately measure all properties of each lobe before making the dimers [24–31].

We first study the propulsion of polystyrene dimers made from 2 and 3 μm spheres with similar zeta potentials ($\zeta = -56$ and -59 mV). As shown in the Supplemental Material [24], Fig. 1, a thin film of particle suspension is sandwiched between two electrodes that are separated by an insulating spacer $\sim$100 μm. When an ac voltage is applied perpendicularly, the asymmetric dimers move laterally on the substrate (Supplemental Material [24], movie 1). In comparison, spheres and symmetric dimers undergo Brownian motion only. The asymmetric dimer propels with its small lobe facing forward when $\omega < 1400$ Hz. It moves towards the opposite direction, i.e., the big lobe facing forward when $1400\ \text{Hz} < \omega < 6000$ Hz. At higher frequencies, the lying dimer changes its orientation and stands on the substrate. Being axial symmetric with respect to the field, the dimer stops its propulsion. Figure 1(a) shows the measured dimer velocity under a constant voltage. Three distinct frequency regimes that show fast propulsion, reverse motion, and orientation change can be identified. Figure 2 in the Supplemental Material [24] shows that the propulsion speed scales linearly with the squared field strength and

 © 2015 American Physical Society

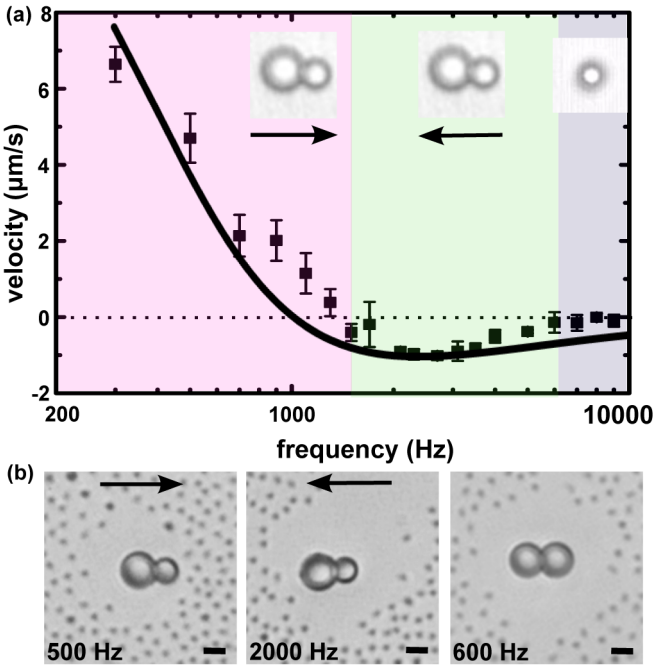

FIG. 1 (color online). (a) The propulsion velocity of a 2–3 μm polystyrene dimer under 6.5 V_p in 10^{-5} M KCl solution. The solid line is a theoretical prediction based on Eq. (3) in the text ($\beta = 0.04$ and $\sigma_{sl} = 5$ nS). The insets show its propulsion directions and orientation. (b) Tracer particles surrounding immobilized asymmetric and symmetric dimers at different frequencies. Scale bars: 2 μm.

inverse of frequency ($U \propto E_0^2/\omega$). The polystyrene dimers made from 1 and 3 μm spheres with similar zeta potentials ($\zeta = -52$ and -59 mV) exhibit qualitatively similar behavior, as summarized in Fig. 3 of the Supplemental Material [24].

Although perpendicular motion relative to the applied field direction has been reported for gold-polystyrene Janus spheres due to ICEO along the gold surface, its flow on dielectric surfaces (e.g., polystyrene here) is negligible and ICEO does not appear to be responsible for the propulsion [14]. It is, however, known that there is an EHD flow surrounding dielectric spheres near a conducting substrate [17,19]. The vertically applied electric field attracts mobile charges towards the substrate. The same field also polarizes the particle, whose induced dipole generates a local field. Its tangential component can drive the induced charges and solvent flow along the substrate. Although the flow surrounding a sphere is symmetric, it can become unbalanced if the particle symmetry is broken. Hence, we hypothesize that the propulsion of polystyrene dimers is caused by an unbalanced EHD flow surrounding them. The fact that spheres, symmetric dimers, and standing asymmetric dimers do not propel under the same experimental conditions is supportive. Moreover, the propulsion velocity scales linearly with E_0^2 and ω^{-1}, which is a characteristic feature of EHD flow as suggested by previous experiments and modeling for spheres [17].

The EHD flow surrounding a dielectric particle depends on the amount of induced charges q near the conducting substrate. If it is small, the EHD flow will be weak. To test this, we investigate the propulsion of polystyrene dimers in a solvent that is less polar than water, i.e., dimethyl sulfoxide (DMSO). Under the same field strength, the dimer moves at ~ 0.1 μm/sec over a wide frequency regime (600 Hz $< \omega <$ 4000 Hz), as compared with $\sim$2–5 μm/sec shown in Fig. 1(a). This decrease of the propulsion speed can be attributed to a much weaker EHD flow in DMSO since the concentration of ions is about 2 orders of magnitude lower than the aqueous solution with 10^{-5} M KCl.

To directly probe the EHD flow surrounding particles, we purposely immobilize them on the substrate and use small fluorescent polystyrene spheres ($\sim$500 nm) as tracers. The Supplemental Material [24], movie 2a, shows the motion of tracers surrounding a 3 μm sphere at two different focus planes. Close to the substrate, tracers are continuously ejected away from the sphere. When the focus plane is ~ 4 μm above the substrate, tracers in the bulk are attracted towards the top of the sphere over long distances. A few of them can even stay closely above the sphere presumably due to dipolar attraction. Combining the tracer motion at different focus planes (Supplemental Material [24], Fig. 4), we reveal a circulating EHD flow that is directed away from the sphere near the substrate and towards the sphere in the bulk. This flow is also captured by our calculation based on the standard electrokinetic model and is counterclockwise if we define a two-dimensional axial symmetric coordinate system shown in the Supplemental Material [24], Fig. 4(c). Because of the repulsive nature of this EHD flow, a circular depletion zone surrounding the sphere can also be seen. When frequency is increased or field strength is decreased, both the ejection speed of tracers and the size of the depletion zone become smaller, indicating a weaker flow. Qualitatively similar flow can also be observed surrounding an asymmetric polystyrene dimer (Supplemental Material [24], movie 2b). More importantly, the depletion zones surrounding the small and large lobes are of different sizes [Fig. 1(b)], indicating different magnitudes of flow. In comparison, the depletion zone surrounding a 3-3 μm dimer is always symmetric. As a result, it does not propel.

To further establish the link between the unbalanced EHD flow and particle motion, we investigate dimers made of silica, e.g., a 2–3 μm silica dimer with similar zeta potentials ($\zeta = -67$ and -64 mV). As shown in the Supplemental Material [24], movie 3a, the asymmetric silica dimer also propels, while the symmetric (2-2 or 3-3 μm) ones do not. Consistent with polystyrene dimers, we find that the propulsion speed is proportional to E_0^2 [Fig. 2(a)] and ω^{-1} (Supplemental Material [24], Fig. 5), which demonstrates the universality of this propulsion mechanism. Nonetheless, the propelling silica dimer

orients its large lobe forward, opposite to what is observed for 2–3 μm polystyrene dimers, at least in the low frequency regime. To find out why, we immobilize the silica dimers and probe the EHD flow surrounding them. To our surprise, tracers move very differently. When the field strength is increased gradually, tracers flow towards the silica dimer (Supplemental Material [24], movie 3b). Some early arrivers even form rings surrounding it. When focusing on the top of the dimer, we observe that tracers are continuously ejected away. Clearly, the EHD flow surrounding an asymmetric silica dimer circulates clockwise. Such an attractive flow also concentrates tracers surrounding the silica dimer, as evidenced in Fig. 2(b) (i). The stark contrast between the concentration zone surrounding a silica sphere and the depletion zone surrounding a polystyrene sphere [Fig. 2(b)] also illustrates the attractive and repulsive nature of EHD flow, respectively. Although we do not know why silica spheres behave so differently from polystyrene spheres, our discovery is significant: when the EHD flow surrounding its constituent spheres changes the direction from counterclockwise to clockwise (i.e., polystyrene vs silica), dimers with the same degree of geometric asymmetry also move in opposite directions. Therefore, our seemingly contradictory results between polystyrene and silica dimers indeed further support our hypothesis that the unbalanced EHD flow surrounding an asymmetric particle dictates its propelling direction.

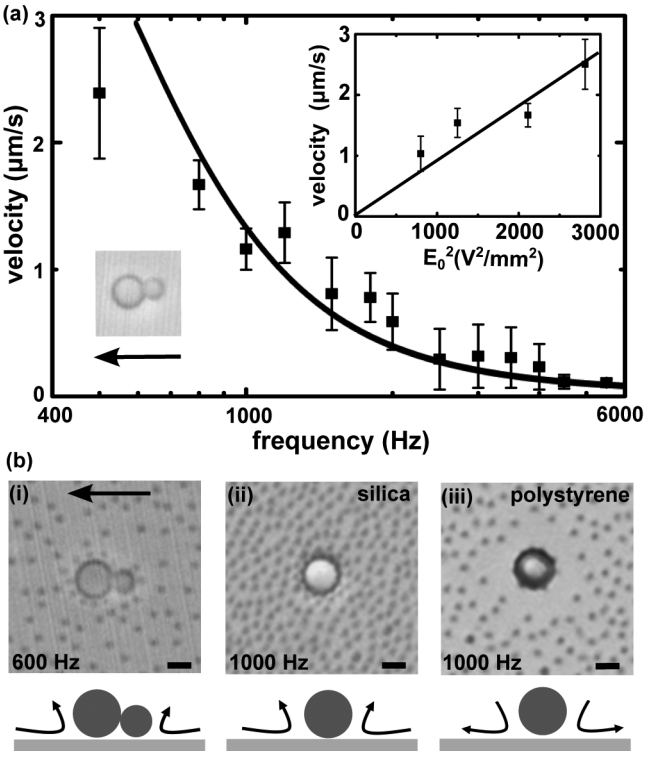

FIG. 2. (a) The propulsion velocity of a 2–3 μm silica dimer under 6.5 V_p in 10^{-5} M KCl solution. The solid line is a theoretical prediction based on Eq. (3) in the text ($\beta = 0.02$ and $\sigma_{sl} = 0.05$ nS). The right inset shows that its velocity scales linearly with field strength squared. (b) Tracer particles surrounding an immobilized (i) silica dimer, (ii) silica sphere, and (iii) polystyrene sphere. Scale bars: 2 μm.

A notable question is whether one can predict the propelling direction and speed of an asymmetric dimer, given the information of EHD flow surrounding its constituent lobes. As an approximation, we consider two spheres A and B, which are connected by a long but thin rod [Fig. 3(a)]. If they are close but not connected, each will move due to its convective entrainment in the EHD flow initiated from the other. For example, the attractive (repulsive) EHD flow surrounding sphere B will draw (push) sphere A towards (away from) it with a lateral velocity U_B. Similarly, sphere B acquires a lateral velocity U_A due to the EHD flow initiated from A. When two spheres are connected, however, equal and opposite forces $\pm F$ on two ends of the rod keep them from moving relative to each other, so that the rigid dumbbell will move with a velocity

$$U = U_B - F/6\pi\mu R_A = U_A + F/6\pi\mu R_B, \qquad (1)$$

where R_A and R_B are radii of spheres A and B, respectively, and μ is the solvent viscosity. Solving F from Eq. (1), we obtain

$$U = (U_B R_A + U_A R_B)/(R_A + R_B). \qquad (2)$$

Although the dumbbell shown in Fig. 3(a) is different from our tangentially touching dimers, their propulsion behavior should be perturbatively similar. Equation (2)

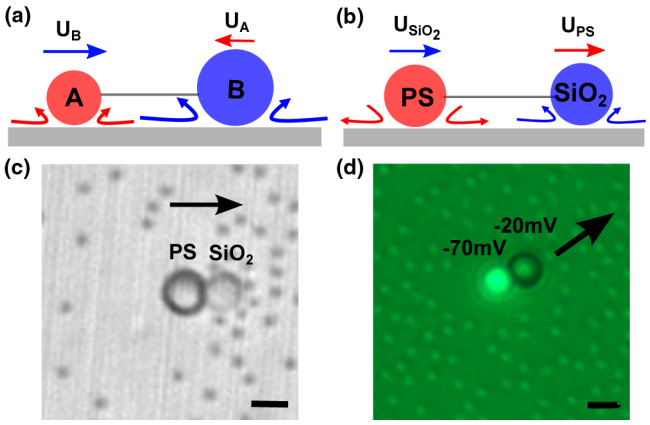

FIG. 3 (color online). (a) A dumbbell model illustrates that the propulsion of an asymmetric dimer arises from unbalanced EHD flow of U_A and U_B. (b) A PS-SiO_2 dimer is predicted to move towards the SiO_2 end. (c) Tracers surrounding an immobilized 2-2 μm PS-SiO_2 dimer. (d) An overlay of bright-field and fluorescent microscopy images shows tracers surrounding an immobilized 2-2 μm polystyrene dimer with asymmetric distribution of zeta potentials. For both (c) and (d), the arrow indicates the dimer's propulsion direction if it is free to move. Scale bar: 2 μm.

allows us to predict the behavior of a propelling dimer. For example, symmetric dimers with identical lobes do not propel because $U_A = -U_B$. For asymmetric dimers, when the EHD flows are repulsive or attractive for both spheres, U_A and U_B are in opposite signs but of different magnitudes. The dimer's propulsion direction and overall velocity will depend on the quantitative difference between $U_B R_A$ and $U_A R_B$, which we will discuss later. When the EHD flow surrounding one lobe is attractive while the other is repulsive, both U_A and U_B point to the same direction, so does U. For example, as illustrated in Fig. 3(b), a hybrid dimer made of polystyrene and silica spheres will propel with the silica lobe facing forward, since we have demonstrated that the EHD flow is repulsive surrounding a polystyrene sphere and attractive surrounding a silica sphere. To test this prediction, we make hybrid dimers from 2 μm silica and 2 μm polystyrene spheres with similar zeta potentials ($\zeta = -67$ and -56 mV). Note that the silica lobe will be more "transparent" than polystyrene in water because of its smaller refractive index. Supplemental Material [24], movie 4, shows clearly that the PS-SiO_2 dimers propel with its silica lobe facing forward and its velocity decreases with increasing frequency (Supplemental Material [24], Fig. 6). Interestingly, we observe a dimer in which silica and polystyrene spheres are linked by a long thread (dust). It closely resembles our dumbbell model in Fig. 3(b) and moves in the same way as our tangentially touching dimers (Supplemental Material [24], movie 4). When immobilizing the PS-SiO_2 dimer, we confirm that tracers are attracted towards the SiO_2 lobe and ejected away from the PS lobe. As a result, they are surrounded by concentration and depletion zones, respectively [Fig. 3(c)]. Therefore, both the propulsion direction and EHD flow profiles of the hybrid dimer are consistent with the simple model in Fig. 3(b).

In addition to geometry and chemical composition, other types of broken symmetry can influence the EHD flow too. For example, our calculation based on the standard electrokinetic model [17] shows that the EHD flow is opposite for spheres of the same composition (e.g., polystyrene) but with different zeta potentials (Supplemental Material [24], Fig. 7), being attractive for low zeta potentials but repulsive for high zeta potentials. This also agrees with previously reported experiments [32]. We therefore make polystyrene dimers that are symmetric in geometry (2 μm), identical in chemical composition, but asymmetric in zeta potentials ($\zeta = -20$ and -70 mV). To distinguish two lobes, one of them (-70 mV) is fluorescently labeled. Based on Eq. (2), one could predict that such a dimer will propel with its low-zeta-potential lobe facing forward. Supplemental Material [24] movie 5 confirms it. The tracer experiments also illustrate the difference in EHD flow between two lobes [Fig. 3(d)]. Therefore, our model is further validated.

To quantitatively predict the propulsion velocity, one needs detailed information of U_A and U_B, which can be estimated based on the following scaling law (see Supplemental Material [24] texts for details) derived from literature [33,34].

$$U_i = \beta \frac{\varepsilon\varepsilon_0 \kappa H}{\mu} \left(\frac{V_p}{2H}\right)^2 \frac{K' + \bar{\omega}K''}{1+\bar{\omega}^2} \frac{3(r/R_i)}{2[1+(r/R_i)^2]^{5/2}}, \quad (3)$$

where $\varepsilon\varepsilon_0$ is the solvent permittivity, κ^{-1} is the Debye length, V_p is the peak voltage, $2H$ is the separation between two electrodes, R_i is the particle radius, and r is the lateral distance from the particle center to the point where the EHD flow is evaluated. β is a prefactor used to relate the scaling velocity of fluid in Eq. (3) to the particle velocity in Eq. (2) for a quantitative comparison with experimental data. The frequency is scaled by the inverse of RC time for charging the electrode $\bar{\omega} = \omega H/\kappa D$ (D is the ion diffusivity), which controls the dynamics of diffusive charges near the substrate. The key parameters in Eq. (3) are K' and K'', the real and imaginary parts of the polarization coefficient, respectively. They, being functions of R_i, ω, κ, ζ, and the Stern-layer conductance σ_{sl}, are calculated analytically based on the Dukhin-Shilov model [35,36]. We note that under typical experimental conditions, $\bar{\omega} \gg 1$ and $K' \propto \omega$. Therefore, the velocity U_i scales with ω^{-1}, which is consistent with our experimental results. By substituting $R_A = 1$ μm, $R_B = 1.5$ μm, $r = R_A + R_B$, and all other relevant parameters into Eq. (3), we obtain the EHD velocities for individual 2 and 3 μm silica spheres, i.e., U_A and U_B in 10^{-5} M KCl solution [Fig. 4(a)], with two fitting parameters of β (0.02) and σ_{sl} (0.05 nS). Corresponding to the schematics in Fig. 3(a), the attractive EHD flow originated from sphere A pulls B towards the left. Therefore, U_A is negative. U_B is positive because sphere B pulls A towards the right. The overall propulsion velocity of the 2–3 μm SiO_2 dimer U can then be calculated by Eq. (2) and is plotted by the solid line in Fig. 4(a), which well matches the experimental data. Similarly, we calculate the EHD velocities for individual 2 and 3 μm polystyrene spheres. Interestingly, we find that a much larger Stern-layer conductance σ_{sl} (5 nS) is necessary for polystyrene spheres than for silica spheres (0.05 nS) in order to predict

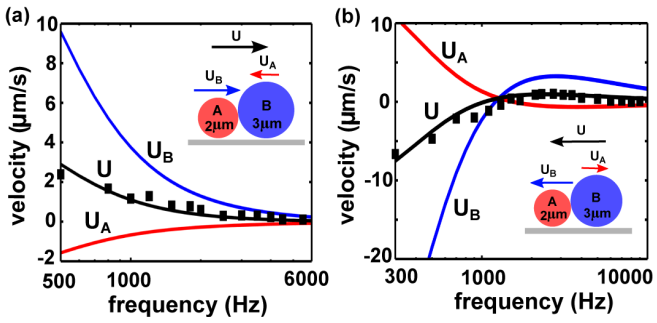

FIG. 4 (color online). Calculated EHD velocities of the (a) 2–3 μm silica dimer ($\beta = 0.02$ and $\sigma_{sl} = 0.05$ nS) and (b) 2–3 μm polystyrene dimer ($\beta = 0.04$ and $\sigma_{sl} = 5$ nS). The squares are experimental results.

its surrounding repulsive EHD flow. Although both values of Stern-layer conductance are within the experimental regime (0.06–10 nS) reported previously [37–40], the surface chemistry and charging mechanism for polystyrene and silica particles are quite different. Therefore, their difference in the Stern-layer conductance could well explain why polystyrene and silica dimers behave so differently although their sizes and zeta potentials are similar. The propulsion velocity of 2–3 and 1–3 μm polystyrene dimers are plotted in the solid lines in Fig. 4(b) and Supplemental Material [24], Fig. 3. It can be seen that the reverse motion on polystyrene dimers is caused by the change of EHD flow directions and magnitudes for both lobes (U_A and U_B) at higher frequencies.

In conclusion, we discover the lateral propulsion of dielectric dimers under a perpendicularly applied ac electric field. Comprehensive evidence shows that asymmetric particle properties in geometry, composition, and surface charge can all influence the EHD flow surrounding two sides of the dimers differently in both flow direction and magnitude. Such a difference results in an unbalanced EHD flow and induces particle motion. Built upon a simple dumbbell model and scaling laws, we quantitatively predict both the propulsion direction and speed of the dimers, which are also validated by experiments. The propulsion mechanism revealed here should be universal for other types of asymmetric particles. Such knowledge is important for both studying the out-of-equilibrium behavior of active matter and building intelligent colloidal robots.

This work was supported by the National Science Foundation under Grant No. CBET-1336893.

*Corresponding author.
ningwu@mines.edu

[1] J. Howard, Nature (London) **389**, 561 (1997).
[2] D. Keller and C. Bustamante, Biophys. J. **78**, 541 (2000).
[3] G. A. Ozin, I. Manners, S. Fournier-Bidoz, and A. Arsenault, Adv. Mater. **17**, 3011 (2005).
[4] J. Wang, Lab Chip **12**, 1944 (2012).
[5] S. Sengupta, M. E. Ibele, and A. Sen, Angew. Chem., Int. Ed. Engl. **51**, 8434 (2012).
[6] V. Magdanz, S. Sanchez, and O. G. Schmidt, Adv. Mater. **25**, 6581 (2013).
[7] H. K. Hunt and A. M. Armani, Nanoscale **2**, 1544 (2010).
[8] R. Fernandes and D. H. Gracias, Mater. Today **12**, 14 (2009).
[9] E. M. Purcell, Am. J. Phys. **45**, 3 (1977).
[10] E. Lauga and T. R. Powers, Rep. Prog. Phys. **72**, 096601 (2009).
[11] T. M. Squires and M. Z. Bazant, J. Fluid Mech. **560**, 65 (2006).
[12] S. Gangwal, O. J. Cayre, M. Z. Bazant, and O. D. Velev, Phys. Rev. Lett. **100**, 058302 (2008).
[13] J. Lyklema, *Fundamentals of Interface and Colloid Science, Solid-Liquid Interfaces* (Academic Press, San Diego, CA, 1995), Vol. 2.
[14] T. M. Squires and M. Z. Bazant, J. Fluid Mech. **509**, 217 (2004).
[15] M. Trau, D. A. Saville, and I. A. Aksay, Science **272**, 706 (1996).
[16] S. R. Yeh, M. Seul, and B. I. Shraiman, Nature (London) **386**, 57 (1997).
[17] W. D. Ristenpart, I. A. Aksay, and D. A. Saville, J. Fluid Mech. **575**, 83 (2007).
[18] C. L. Wirth, R. M. Rock, P. J. Sides, and D. C. Prieve, Langmuir **27**, 9781 (2011).
[19] D. C. Prieve, P. J. Sides, and C. L. Wirth, Curr. Opin. Colloid Interface Sci. **15**, 160 (2010).
[20] F. Ma, S. Wang, L. Smith, and N. Wu, Adv. Funct. Mater. **22**, 4334 (2012).
[21] T. Y. Gong, D. T. Wu, and D. W. M. Marr, Langmuir **18**, 10064 (2002).
[22] F. Ma, S. Wang, D. T. Wu, and N. Wu, Proc. Natl. Acad. Sci. U.S.A. **112**, 6307 (2015).
[23] A. M. Yake, R. a. Panella, C. E. Snyder, and D. Velegol, Langmuir **22**, 9135 (2006).
[24] See Supplemental Material http://link.aps.org/supplemental/10.1103/PhysRevLett.115.208302 for experimental procedures, additional measurement, and details for modeling, which includes Refs. [25–31].
[25] A. V. Delgado, F. Gonzalez-Caballero, R. J. Hunter, L. K. Koopal, and J. Lyklema, J. Colloid Interface Sci. **309**, 194 (2007).
[26] M. D. Abramoff, P. J. Magalhães, and S. J. Ram, Biophotonics Intl. **11**, 36 (2004).
[27] J. R. Howse, R. A. L. Jones, A. J. Ryan, T. Gough, R. Vafabakhsh, and R. Golestanian, Phys. Rev. Lett. **99**, 048102 (2007).
[28] T. B. Jones, *Electromechanics of Particles* (Cambridge University Press, Cambridge, England, 1995), p. 288.
[29] H. Zhou, M. A. Preston, R. D. Tilton, and L. R. White, J. Colloid Interface Sci. **285**, 845 (2005).
[30] J. G. V. Bladel, *Electromagnetic Fields*, 2nd ed. (John Wiley & Sons, Inc, Hoboken, NJ, 2007), p. 1028.
[31] S. J. Wang, F. D. Ma, H. Zhao, and N. Wu, ACS Appl. Mater. Interfaces **6**, 4560 (2014).
[32] T. J. Woehl, K. L. Heatley, C. S. Dutcher, N. H. Talken, and W. D. Ristenpart, Langmuir **30**, 4887 (2014).
[33] F. D. Ma, S. J. Wang, H. Zhao, D. T. Wu, and N. Wu, Soft Matter **10**, 8349 (2014).
[34] W. D. Ristenpart, I. A. Aksay, and D. A. Saville, Phys. Rev. E **69**, 021405 (2004).
[35] S. Dukhin and V. N. Shilov, *Dielectric Phenomena and the Double Layer in Disperse Systems and Polyelectrolytes* (Wiley, New York, 1974).
[36] V. N. Shilov, A. V. Delgado, F. Gonzalez-Caballero, and C. Grosse, Colloids Surf. A **192**, 253 (2001).
[37] L. Collins, J. I. Kilpatrick, S. A. L. Weber, A. Tselev, I. V. Vlassiouk, I. N. Ivanov, S. Jesse, S. V. Kalinin, and B. J. Rodriguez, Nanotechnology **24**, 475702 (2013).
[38] M. Kappl and H.-J. Butt, Part. Part. Syst. Charact. **19**, 129 (2002).
[39] B. W. Kwaadgras, T. H. Besseling, T. J. Coopmans, A. Kuijk, A. Imhof, A. v. Blaaderen, M. Dijkstra, and R. v. Roij, Phys. Chem. Chem. Phys. **16**, 22575 (2014).
[40] M. Mijalkov and G. Volpe, Soft Matter **9**, 6376 (2013).